Molecular Therapy
Nucleic Acids
Brief Report

AAV-based gene editing of type 1 collagen mutation to treat osteogenesis imperfecta

Yeon-Suk Yang,[1] Tadatoshi Sato,[1,2,5,6] Sachin Chaugule,[1] Hong Ma,[2,3,4] Jun Xie,[2,3,4] Guangping Gao,[2,3,4,5] and Jae-Hyuck Shim[1,2,5]

[1]Department of Medicine, Division of Rheumatology, UMass Chan Medical School, Worcester, MA 01655, USA; [2]Horae Gene Therapy Center, UMass Chan Medical School, Worcester, MA 01655, USA; [3]Department of Microbiology and Physiological Systems, UMass Chan Medical School, Worcester, MA 01655, USA; [4]Viral Vector Core, UMass Chan Medical School, Worcester, MA 01655, USA; [5]Li Weibo Institute for Rare Diseases Research, UMass Chan Medical School, Worcester, MA 01655, USA; [6]Endocrine Unit, Massachusetts General Hospital, Harvard Medical School, Boston, MA 02114, USA

Osteogenesis imperfecta (OI) is a genetic disorder characterized by bone fragility, low bone mass, fractures, and extraskeletal manifestations. Since OI is commonly caused by single-nucleotide mutation(s) in the *COL1A1* or *COL1A2* genes encoding type I collagens, we developed a genome-editing strategy to correct a *Col1a2* mutation in an OIM mouse model resembling a severe dominant form of human type III OI. Using a recombinant adeno-associated virus (rAAV), we delivered CRISPR-Cas9 to bone-forming osteoblast-lineage cells in the skeleton. Homology-directed repair (HDR)–mediated gene editing efficiency in these cells was improved when CRISPR-Cas9 was coupled with a donor AAV vector containing a promoterless partial mouse *Col1a2* complementary DNA sequence. This approach effectively reversed the dysregulation of osteogenic differentiation by a *Col1a2* mutation *in vitro*. Furthermore, systemic administration of dual rAAVs in OIM mice lowered bone matrix turnover rates by reducing osteoblast and osteoclast development while improving the cellular network of mechano-sensing osteocytes embedded in the bone matrix. This strategy significantly improved bone architecture/mass/mineralization, skeletal deformities, grip strength, and spontaneous fractures. Our study is the first demonstration that HDR-mediated gene editing via AAV-mediated delivery effectively corrects a collagen mutation in OI osteoblasts and reverses skeletal phenotypes in OIM mice.

INTRODUCTION

Osteogenesis imperfecta (OI) is a genetic disorder with an incidence of ~1 in 10,000–20,000.[1] The disease is characterized by bone fragility and dysplasia, low bone mass, recurrent bone fractures following minor trauma, bowing of the long bones, vertebral compression, scoliosis, bone pain, stunted growth, and ligamentous and joint laxity.[2] Approximately 85% of OI patients have autosomal dominant mutations in the *COL1A1* or *COL1A2* genes that encode the α1 or α2 chains, respectively, of type I collagen, the major structural protein of bone. Other OI patients have dominant, recessive, or X-linked mutations in the genes associated with collagen synthesis, processing, or crosslinking.[2,3] Current treatments include surgical intervention with intramedullary stabilization and the use of prostheses, as well as pharmacological agents that are mostly borrowed from those developed to treat osteoporosis or osteolytic bone metastasis and their complications. However, these drugs show limited success in the clinic since they are unable to alter the source of the collagen mutations.[3,4]

Gene therapy has recently emerged as a promising therapeutic tool to treat genetic disorders by repairing mutations in the locus. Since the majority of OI patients have autosomal dominant mutations in the *COL1A1* or *COL1A2* genes, several attempts in OI mutant allele-specific suppression have been made using various RNAi technologies such as antisense oligonucleotides, ribozymes, and small interfering RNA (siRNA).[5,6] Nonviral vectors such as nanoparticles, liposomes, and lipid nanoparticles (LNPs) were used to deliver RNAi to target cells and tissues.[7] Despite promising data in *in vitro* and *ex vivo* studies, the systemic delivery of RNAi is less effective for knockdown and targeting specificity to bone or bone-residing cells *in vivo*. In addition, nonviral vectors can be rapidly degraded *in vivo*, cleared in the circulation, have short biological half-lives, and generally exhibit nonspecific uptake to cells.[7] An alternative delivery modality is a viral vector, such as recombinant adeno-associated virus (rAAV). rAAV has a long track record for safety and efficacy in relevant preclinical and clinical studies[8] while demonstrating high transduction efficiency, persistent transgene expression, and lack of postinfection immunogenicity and pathogenicity.[9] Recently, rAAV9 has been identified as a highly effective serotype for the transduction of osteoblast-lineage cells and a single dose of intravenous (i.v.) administration of rAAV9 enables long-lasting expression of artificial microRNA (miRNA) in skeleton.[10,11]

https://doi.org/10.1016/j.omtn.2023.102111.

Correspondence: Dr. Jun Xie, Horae Gene Therapy Center, UMass Chan Medical School, Worcester, MA 01655, USA.
E-mail: jun.xie@umassmed.edu
Correspondence: Dr. Guangping Gao, Horae Gene Therapy Center, UMass Chan Medical School, Worcester, MA 01655, USA.
E-mail: guangping.gao@umassmed.edu
Correspondence: Dr. Jae-Hyuck Shim, Department of Medicine/Division of Rheumatology, UMass Chan Medical School, Worcester, MA 01655, USA.
E-mail: jaehyuck.shim@umassmed.edu

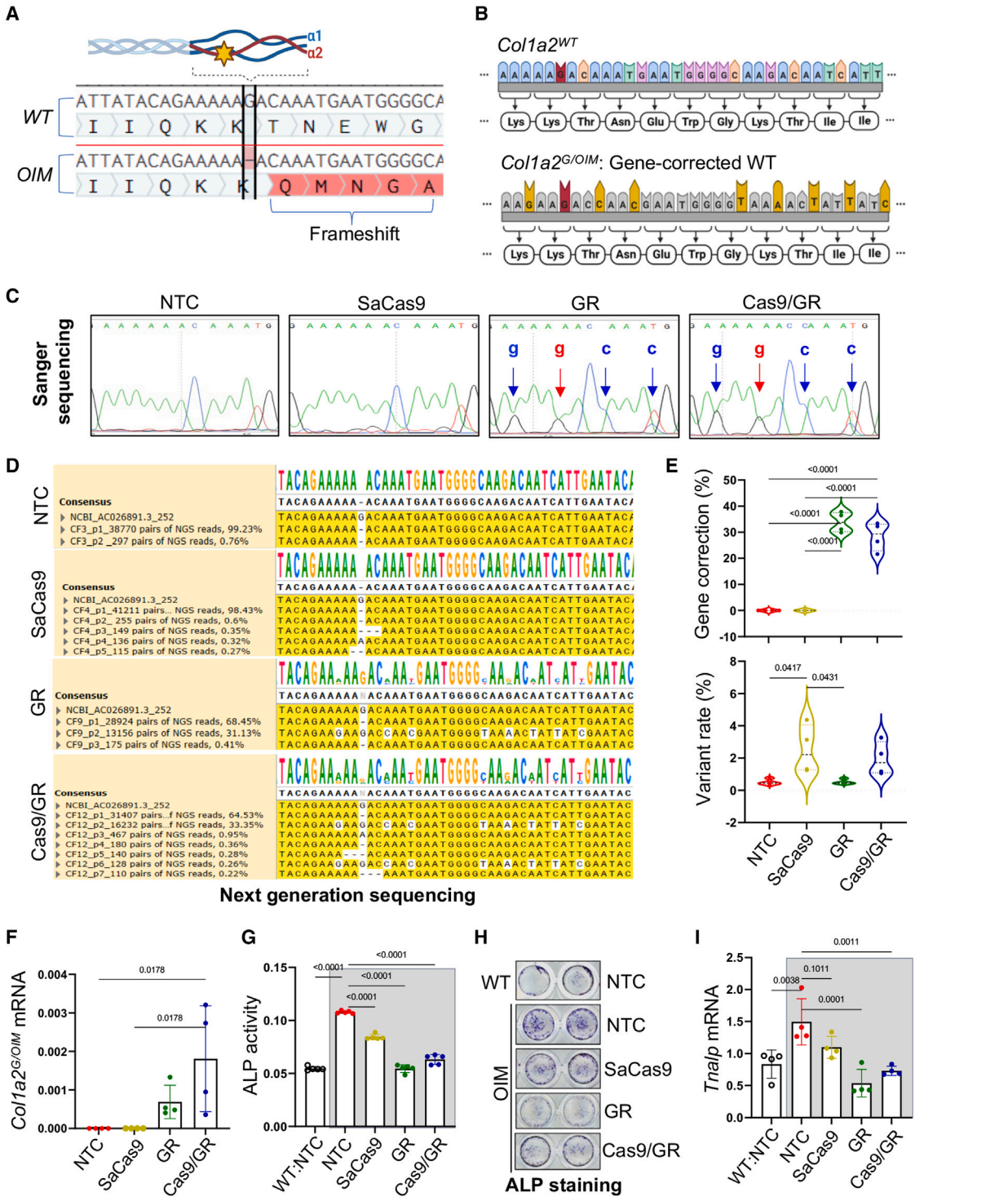

Figure 1. AAV-mediated *Col1α2* gene correction in OIM osteoblasts

(A) Schematic diagram showing a frameshift mutation in the *Col1α2* gene of homozygous OIM (OIM) mice. Deletion of a guanine (G) at nucleotide 3,983 of the *Col1α2* gene induces a frameshift of ~50 terminal amino acids of the pro-α2 C-terminal propeptide domain. (B) Schematic diagram shows the repairing template sequences of pro-α2 C-terminal propeptide domain. Eight nucleotides were replaced as codon optimization to stabilize the corrected Col1α2 protein expression. (C–E) Immortalized OIM osteoblasts were treated with rAAV9s carrying NTC, sgRNA + SaCas9 (SaCas9), GeneRide (GR), or sgRNA + SaCas9 + GeneRide (Cas9/GR), and 3 days later, genomic DNA

(legend continued on next page)

Unlike RNAi therapies with transient therapeutic efficacy, the CRISPR-CRISPR-associated protein 9 (Cas9) system shows long-term therapeutic effects in the gene edited cells. The CRISPR-Cas9 system has been developed as a genome-editing tool that can correct DNA mutations. In principle, many heterozygous mutations can be individually corrected by homology-directed repair (HDR) using an exogenous DNA template.[12–14] As a gene therapy vector, LNPs have been developed for the delivery of Cas9 plasmid DNA, mRNA, and ribonucleoproteins.[15,16] However, they are limited in their use of *in vivo* gene editing due to low delivery efficiency, although they have an advantageous safety profile compared to viral vector approaches. Given that CRISPR-Cas9-mediated gene therapy shows off-target cleavage and mutagenesis by nonhomologous end joining (NHEJ) and poor efficiency by HDR,[14] a nuclease-free gene editing strategy GR (GeneRide) that can insert a promoterless complementary DNA sequences into targeted genes has also been developed.[17] Although AAV-mediated delivery of Cas9 and a single-guide RNA (sgRNA) in mouse liver and muscle has proven successful,[18–20] AAV-mediated delivery of GeneRide enabled the targeted insertion of human coagulation factor IX gene into the liver-expressed mouse albumin locus, ameliorating hemophilia B in mice.[17] Here, we demonstrated that a systemic delivery via rAAV9 corrects a frameshift mutation in the *Col1a2* gene in a mouse model for OI using gene editing strategies via CRISPR-Cas9, GeneRide, or the combination. Systemic delivery of dual AAV9 vectors carrying CRISPR-Cas9 and a promoterless partial mouse *Col1a2* cDNA (GeneRide) corrected the *Col1a2* mutation in OI osteoblasts via HDR, which ameliorates aberrant osteogenic differentiation and osteocyte networking in the bone matrix of OIM mice, thereby dampening high bone turnover rates. Accordingly, these mice show a significant improvement in osteoporosis, skeletal deformities, grip strength, and spontaneous fractures. Thus, our proof-of-concept study demonstrates that an *in vivo* gene editing strategy using a bone-directed AAV may be a promising therapeutic approach for OI.

RESULTS

Strategies for *Col1α2* gene correction in OIM mice

To examine the AAV-mediated gene-editing efficiency to correct a mutation in type I collagen, we used an OI mouse model (OIM mice) harboring the deletion of a guanine (G) at nucleotide 3983 of the *Col1α2* gene, which induces a frameshift of the ∼50 terminal amino acids of the pro-α2 C-terminal propeptide, resulting in the accumulation of abnormal homotrimeric type I collagen in the extracellular matrix[21,22] (Figures 1A and S1A). Homozygous OIM mice show characterized features of OI, such as small body size, progressive skeletal deformities, low bone mass, spontaneous fractures, and poor biomechanical properties.[23,24] The OIM mutation and its biological consequences in homozygous OIM mice are strikingly similar to those found in patients with a severe, nonlethal, and receive form of type III OI.[24] Although OIM mice harbor one nucleotide deletion in the *Col1α2* gene, a four nucleotide deletion (c.4001_4004del) in OI patients induces a frameshift of 33 terminal amino acids of the pro-α2 C-terminal propeptide (p.(Asn1334Serfs*34)). Both of these mutations result in the synthesis of nonfunctional pro-COL1A2, thereby accumulating abnormal homotrimeric type I collagen.[21] Given that AAV-mediated delivery of Cas9 and sgRNA has been reported successfully in mouse liver and muscle *in vitro* and *in vivo*,[18–20] we hypothesized that the systemic delivery of CRISPR-Cas9 to bone-residing osteoblasts via rAAV9[10,11] would correct the OIM mutation. Therefore, we constructed a plasmid that expresses *Staphylococcus aureus*–derived SaCas9 nuclease, which fits within the genome packaging limits of AAV (∼4.85 kb, including both inverted terminal repeats),[25] and an sgRNA sequence targeting a protospacer adjacent motif (PAM) at nucleotides 3,987–3,992 under the transcriptional control of the U1a and U6 promoters, respectively (Figure S1B). Alternatively, the GeneRide strategy[17] enables the correction of the OIM mutation via the targeted insertion of a promoterless partial mouse *Col1a2* cDNA sequences without a nuclease. We therefore constructed a plasmid containing the 1,838-bp-sized complementary sequence to the pro-α2 C-terminal propeptide (810 bp intron, 147 bp exon including G3983 and stop codon, and 881 bp 3′ UTR), and 131-bp SV40 polyadenylation sequence (Figure S1B). The plasmids were packaged into the AAV9 capsid (hereafter referred to as AAV9.SaCas9 and AAV9.GR) to transduce to osteoblast-lineage cells *in vitro* and *in vivo*. To further increase AAV-mediated gene editing efficacy, we combined the GeneRide strategy with the CRISPR-Cas9 platform by simultaneously delivering two AAV9 vectors to OIM osteoblasts *in vitro* and *in vivo* (AAV9.Cas9/GR). An AAV9 carrying a nontargeting control (NTC), AAV9.NTC, was used as a negative control.

AAV-mediated gene editing in OIM osteoblasts

Since the heterogeneity of primary OIM osteoblasts may cause variations in gene editing efficiency, calvarial osteoblasts (COBs) isolated from homozygous OIM (OIM) newborn pups were immortalized by expressing a heat-sensitive SV40 large T antigen and clonally selected to obtain a homogeneous cell population (Figure S2A). AAV-mediated expression and subcellular localization of SaCas9 in OIM osteoblasts were confirmed by qPCR (Figure S2B) and immunofluorescence (Figure S2C) analyses, respectively. Three days after treatment with rAAV9 carrying NTC, sgRNA + SaCas9 (SaCas9), GeneRide (GR), or sgRNA + SaCas9 + GeneRide (Cas9/GR), genomic DNA was isolated from the cells, PCR amplified, and subjected to Sanger sequencing (Figures 1C and S2D) or next-generation

was extracted and subjected to Sanger sequencing (C) or NGS (D and E) analysis (n = 4). GR or Cas9/GR restored the missing "G" (red) in the *Col1α2* gene, and 3 nucleotides (blue) were adapted from GR. The percentage of sequence reads of *Col1α2* gene correction (E, top) or variants (E, bottom) are displayed. (F) mRNA levels of the corrected *Col1α2* gene (*Col1α2*$^{G/OIM}$) in AAV-treated OIM osteoblasts were assessed by qPCR analysis and normalized to β-actin (n = 4). (G–I) Primary osteoblasts isolated from OIM or littermate control (WT) mice were treated with AAV vectors and cultured under osteogenic conditions. Six days later, ALP activity (G and H) and osteogenic gene expression (I) were analyzed (n = 4). WT:NTC indicates WT osteoblasts treated with rAAV9.NTC. Gray boxes: OIM osteoblasts treated with the indicated rAAV9s. Values represent mean ± SD by 1-way ANOVA test (E–G and I).

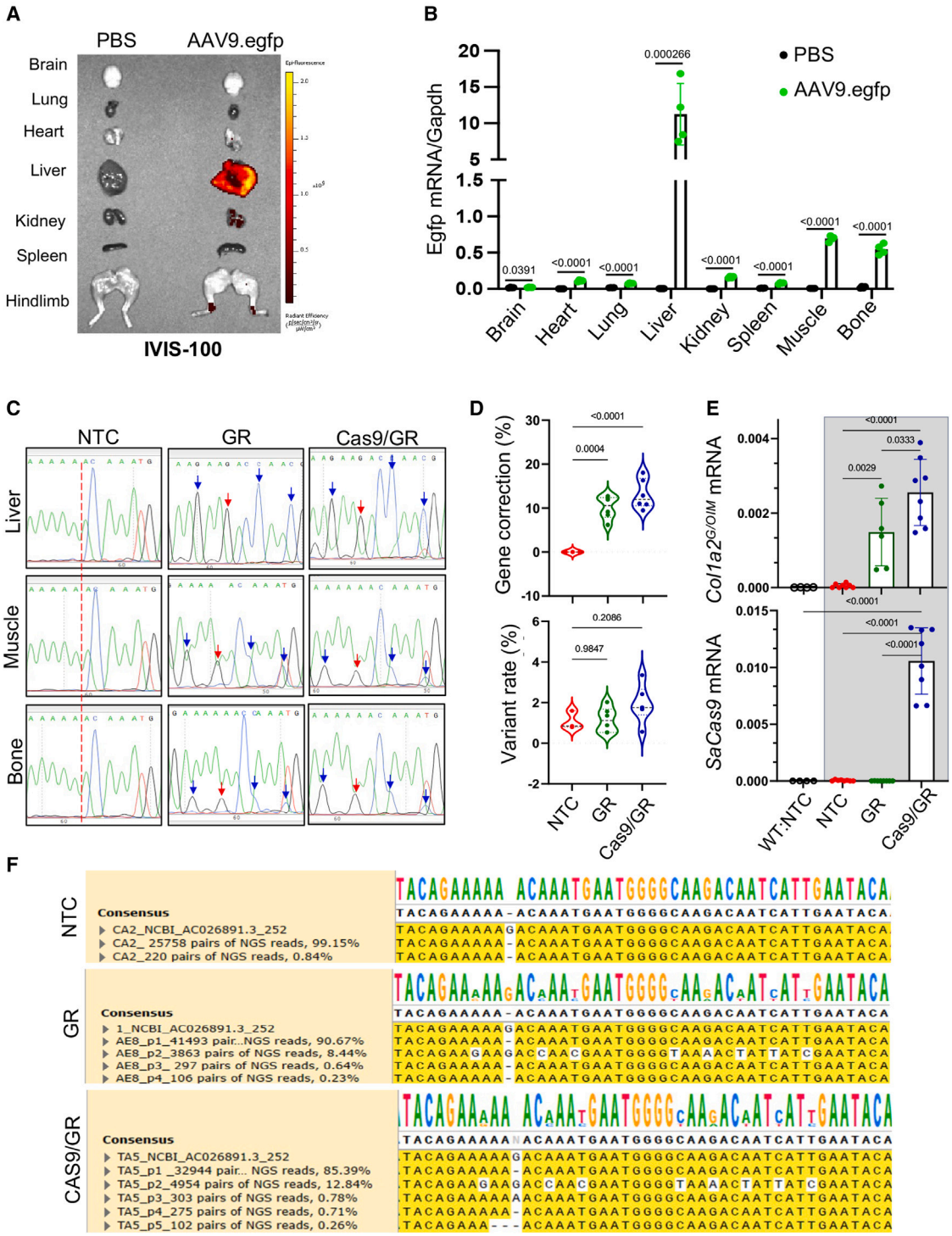

Figure 2. AAV-mediated *Col1α2* gene correction in OIM mice

(A and B) A single dose of PBS or rAAV9.*egfp* (2.5×10^{13} vg/kg) was i.v. injected into 1-month-old OIM mice, and EGFP expression in individual tissues was monitored by IVIS-100 optical imaging 4 weeks postinjection (A). y axis, radiant efficiency (p/s/cm^2/sr/μW/cm^2). Alternatively, protein levels of EGFP in individual tissues were assessed by qPCR (n = 4, B). (C–F) A single dose of rAAV9 carrying NTC, GR, or Cas9/GR (2.5×10^{13} vg/kg) was i.v. injected into 1-month-old OIM mice, and 4 weeks later, genomic DNA was extracted from the liver, muscle, or tibia and subjected to Sanger sequencing (C) or NGS (D and F) analysis (n = 6). The red arrow indicates restoration of the missing "G"

(legend continued on next page)

sequencing (NGS; Figure 1D) to determine *Col1α2* gene correction efficiency in OIM osteoblasts (Figure 1B). Protein expression of Col1α2 in OIM osteoblasts was confirmed by immunoblotting analysis (Figure S3A). NGS analysis of sequence reads revealed that ∼30% of the edited genomes in GR- or Cas9/GR-treated cells carried insertions of the missing guanine (G) in the *Col1α2* gene via HDR, whereas treatment with Cas9/GR or SaCas9 resulted in <1% of adenine insertions via NHEJ (Figures 1D and 1E). The variant frequency analysis showed that the number of reads with gaps in any nucleotide positions near SaCas9-induced cuts reached ∼2% in SaCas9- or Cas9/GR-treated cells relative to NTC- or GR-treated cells showing noise signals (Figure 1E). Expression of the resultant *Col1α2* (*Col1α2*$^{G/OIM}$) mRNA in AAV-treated cells corresponds to higher on-target gene correction efficiency of AAV9 vectors carrying GR than SaCas9, which was further increased in the combination of GR and SaCas9 (Figure 1F). It has been reported that low bone mass in OI results from the dysregulation of osteogenic activity rather than the incapacity of osteoblasts to produce enough organic bone matrix proteins.[26] To test the ability of AAV to reverse dysregulated osteogenic differentiation of OIM osteoblasts, bone marrow–derived stromal cells (BMSCs) were isolated from OIM or littermate control (wild type [WT]) mice, treated with rAAV9s, and cultured under osteogenic conditions. Six days after the culture, early osteoblast differentiation markers, alkaline phosphatase (ALP) activity and tissue nonspecific alkaline phosphatase (Tnalp) expression, were examined (Figures 1G–1I). ALP activity and *Tnalp* expression were markedly elevated in control-treated OIM BMSCs relative to control-treated WT BMSCs, which was almost completely reversed by treatment with GR or Cas9/GR. SaCas9-treated cells showed only a mild reduction. Thus, GR- or Cas9/GR-mediated HDR is more effective for *Col1α2* gene correction in OIM osteoblasts than SaCas9-mediated NHEJ, thereby ameliorating dysregulated differentiation of OIM osteoblasts.

In vivo gene editing in OIM mice

To test whether systemically delivered AAV9 can transduce type I collagen-producing osteoblasts in the skeleton, we assessed the biodistribution of AAV in individual tissues by GFP expression. One-month-old OIM mice were injected i.v. with PBS or rAAV9 expressing GFP protein under the U1a promoter control (AAV9.egfp), and 1 month later, GFP expression in individual tissues was examined by IVIS-100 optical imaging system, qPCR analysis, and fluorescence microscopy in cryo-sectioned tissues (Figures 2A, 2B, and S4). These results demonstrated a high expression in the liver, a modest expression in skeletal muscle and bone, and little to no expression in the brain, heart, lung, kidney, and spleen. Next, OIM mice or littermate controls (WT) were injected i.v. with a single dose of rAAV9 carrying NTC, GR, or Cas9/GR, and 1 month later, genomic DNA was isolated from AAV-transduced liver, skeletal muscle, and femur and subjected to Sanger sequencing or NGS analysis. Since the liver is a major rAAV9-transduced tissue when systemically administered,[27] i.v. administration of rAAV9 carrying GR or Cas9/GR was most effective for *Col1α2* gene correction in the liver relative to skeletal muscle or femur showing a modest transduction efficiency (Figure 2C). Protein expression of Col1α2 in OIM liver was confirmed by immunoblotting analysis (Figure S3B). NGS analysis of sequence reads showed that ∼8% (GR) and 12% (Cas9/GR) of the edited genomes in AAV-treated femurs carried insertions of the missing guanine (G) in the *Col1α2* gene via HDR, whereas Cas9/GR showed <1% of adenine insertions via NHEJ (Figures 2D, 2F, and S5). Sanger sequencing analysis was performed in ∼1.2-kb junctional sequences of endogenous *Col1α2* gene and GeneRide, confirming that the gene editing events primarily occurred within the *Col1α2* gene (Figure S6). Further investigation using whole-genome sequencing is needed to analyze the off-target events of GR- and Cas9/GR-mediated gene editing. Notably, the number of reads with variant sequences reached ∼2% in Cas9/GR-treated femurs relative to NTC- or GR-treated femurs showing noise signals (Figure 2D). The resultant *Col1α2* (*Col1α2*$^{G/OIM}$) expression was also markedly elevated in GR-treated femurs compared to NTC-treated femurs, which was further increased when combined with CRISPR-Cas9 and GR (Figure 2E). Collectively, we showed that systemic delivery of rAAV9 in OIM mice could correct the *Col1α2* mutation in bone-forming osteoblasts via GR- or Cas9/GR-mediated HDR. The combination approach of CRISPR-Cas9 and GR is more effective for *in vivo Col1α2 gene* correction than GR alone.

Col1α2 gene correction in OIM mice ameliorates skeletal phenotypes

It has been reported that OIM neonates at birth often display hemorrhages into joint cavities, visible fractures in the long bones, and a "drooping wrist" appearance due to subluxation on one or both forepaws at different degrees of severity. At the age of 1 month, spontaneous fractures, low bone mass, and deformities of long bones, pelvic bones, and calcaneus bones are also found in these mice.[23] To examine the ability of systemically delivered AAV to reverse OI skeletal phenotypes, 1-month-old OIM mice were i.v. injected with dual rAAV9s expressing SaCas9 and GR (AAV9.Cas9/GR), and 2 months later, a full phenotypic characterization of these mice, including skeletal deformities, spontaneous fractures, grip strength, and bone mass, was performed. Radiographic analysis of the whole body of NTC-treated OIM mice demonstrated a high incidence of fractures with persistent nonunions or abnormal fracture healing in the humerus, femur, and tibia and skeletal deformities in calcaneus and olecranon. These phenotypes were substantially ameliorated by a single dose of rAAV9.Cas9/GR (Figures 3A, 3B, and S7A). Cas9/GR-treated mice also showed an increased ratio of interfemoral distance to interischia distance in the pelvis, suggesting a significant improvement of skeletal deformities in OIM pelvic bone (Figure 3C, top). In addition, the grip strength of these mice was increased, as shown by the greater

(red) in the *Col1α2* gene, and blue arrows indicate 3 nucleotides adapted from GR. The percentage of sequence reads of *Col1α2* gene correction (D, top) or variants (D, bottom) are displayed. Alternatively, total RNA was extracted from the tibia, and expression of the corrected *Col1α2* gene (*Col1α2*$^{G/OIM}$) and SaCas9 nuclease was assessed by qPCR analysis and normalized to β-actin (n = 4–8, E). Gray boxes: OIM mice treated with the indicated rAAV9s. Values represent mean ± SD by an unpaired 2-tailed Student's t test (B) and 1-way ANOVA test (D and E).

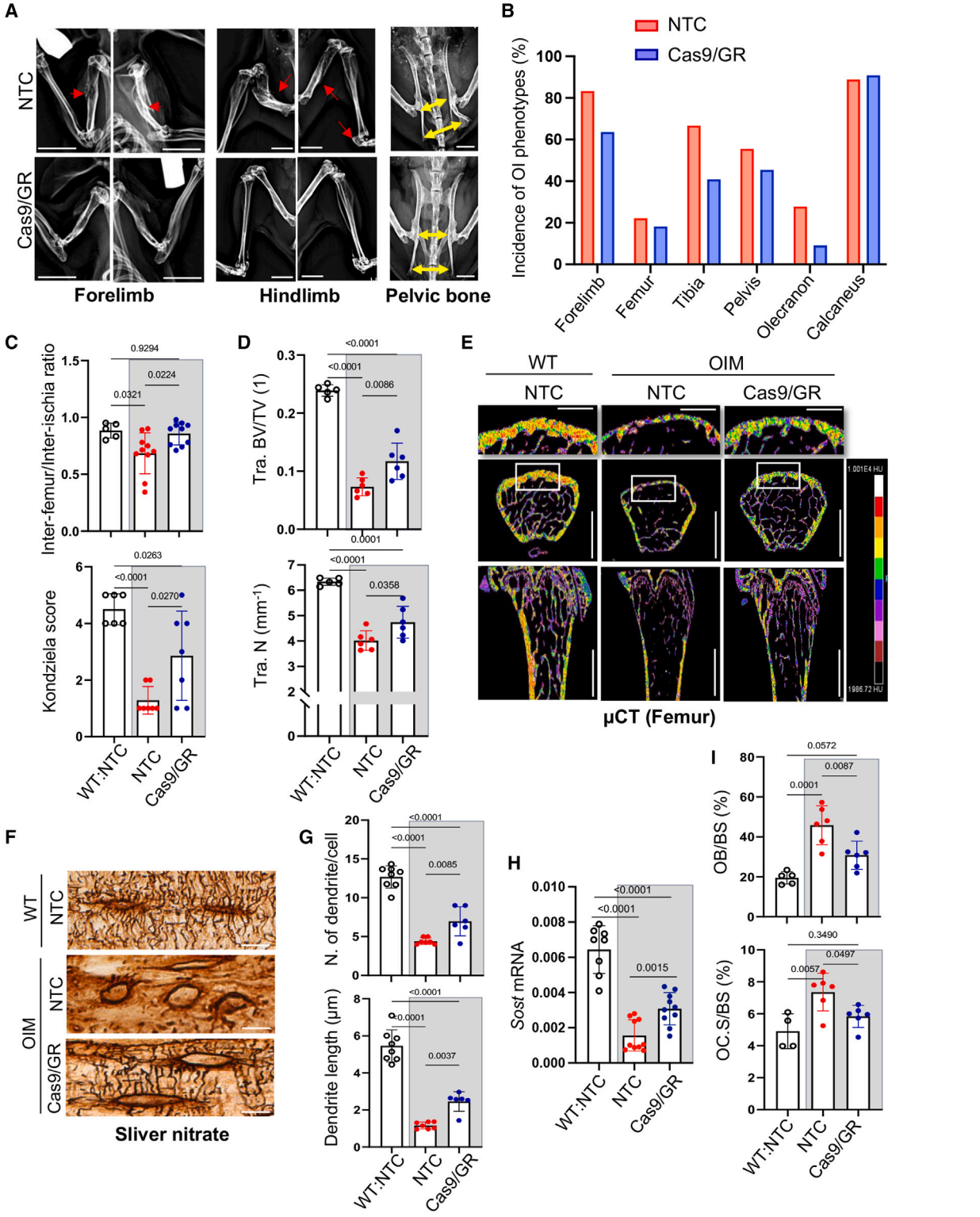

Figure 3. AAV-mediated *Col1α2* gene correction ameliorates OI skeletal phenotypes in OIM mice

A single dose of AAV9 carrying NTC or Cas9/GR (2.5×10^{13} vg/kg) was i.v. injected into 1-month-old WT (n = 5) or OIM (n = 10) mice, and 8 weeks later, radiography of the whole body was performed to locate fractures and skeletal deformities (red arrows, A), and the percentage of their incidence was scored (B), Scale bars, 10 μm. In addition,

(legend continued on next page)

Kondziela score[28,29] (Figure 3C, bottom). Finally, microcomputed tomography (microCT) analysis demonstrated a significant increase in trabecular bone mass and cortical thickness of Cas9/GR-treated femurs relative to NTC-treated femurs (Figures 3D and 3E). Thus, a single dose of systemically delivered rAAV9 expressing Cas9/GR partly reversed OI skeletal phenotypes in OIM mice, including improvements in fracture healing, bone mass, and grip strength along with reduced skeletal deformities.

OI bone is characterized by bone fragility due to abnormal processing and/or synthesis of type I collagen, followed by decreased bone mineral density. These characteristics could affect mechano-sensing networks of osteocytes residing within the mineralized bone matrix that are critical for maintaining bone remodeling and minerals. Compared to NTC-treated WT femurs, NTC-treated OIM femurs display disorganized bone architecture and extracellular matrix deposition (Figure S7B), accompanied by cuboidal-shaped morphology of osteocytes and decreased number and length of osteocyte dendrites (Figures 3F and 3G). In addition, the expression of sclerostin, a marker of mature osteocytes, was markedly reduced, demonstrating a lack of mature osteocytes in the bone matrix of OIM mice (Figure 3H). Notably, *in vivo* osteogenesis and osteoclastogenesis in NTC-treated OIM femurs were both upregulated, resulting in high bone matrix turnover (Figure 3I). When systemically administered with rAAV9.Cas9/GR, bone architecture and extracellular matrix deposition, osteocyte morphology, dendrites, and number, and high bone turnover rates were partly reversed (Figures 3E–3I and S7B).

To examine the durability of systemically delivered rAAV9.Cas9/GR in OIM mice, gene editing efficiency in the femurs was assessed 5 months after AAV injection. AAV-treated femurs showed that ~10% of the edited genomes carried insertions of the missing guanine (G) in the *Col1α2* gene via HDR (Figure S8A). OI skeletal phenotypes in these mice were improved accordingly (Figure S8B). However, further investigation with longer durations (12 or 18 months post-AAV injection) is needed to clarify the durability of AAV in the skeleton. An AAV-mediated gene editing approach that enables correction of the *Col1α2* mutation in OI osteoblasts is a promising strategy to treat disabling OI, providing the potential for clinical translation to OI patients.

DISCUSSION

AAV gene therapy is a promising strategy for treating patients with OI due to the highly recurrent genetic mutation(s) in type I collagens, the lifelong progression of the severe bone fragility and loss throughout the whole body, and the high burden of taking a lifelong medication. In this study, we developed three AAV-based gene editing approaches for OI, including (1) NHEJ-mediated gene correction by CRISPR-Cas9, (2) HDR-mediated gene correction by GeneRide, and (3) HDR-mediated gene correction by the combination of CRISPR-Cas9 and GeneRide. NHEJ is a primary gene editing form of CRISPR-Cas9 that creates small indels. In AAV-treated OIM osteoblasts, CRISPR-Cas9 showed a low gene correction efficiency while producing ~2% variant sequence reads, which may cause potential off-target events. To minimize off-target events and enhance HDR-mediated gene editing by CRISPR-Cas9, further improvements are needed by using base editing[30] or prime editing[31] via other CRISPR-associated nucleases, such as Cpf1[32] or Cas9-nickase,[33] that can increase the efficiency of precise gene editing. However, current forms of base/prime editing are limited in the use of C→T or A→G substitutions, which is not suitable for the OIM mutation. Compared to CRISPR-Cas9-mediated gene editing, HDR-mediated gene correction by GeneRide or Cas9/GR was improved up to ~30% in OIM osteoblasts and ~10% in OIM femurs, demonstrating higher gene correction efficiency by GeneRide alone or the combination of CRISPR-Cas9 and GeneRide than CRISPR-Cas9 alone. Notably, although gene correction rates at genomic levels are comparable between GeneRide alone and the combination, mRNA levels of the corrected *Col1α2* gene were markedly increased by treatment with the combination compared to GeneRide. This discrepancy may result from the inability of NGS primers to distinguish *Col1α2* sequences in genomic DNA versus residual GeneRide. When treated with dual rAAV9s, CRISPR-Cas9 creates double-stranded DNA breaks (DSBs) near nucleotide 3,983 of the *Col1α2* gene in OIM osteoblasts (Figures 1A and 1B), and provision of a promoterless partial mouse *Col1a2* cDNA sequence (GeneRide) drives HDR-mediated gene correction. Alternatively, DSBs created by CRISPR-Cas9 can facilitate the targeted insertion of GeneRide into the *Col1α2* gene.

Treatment of OIM osteoblasts with GeneRide or Cas9/GR restored the missing guanine (G) in the *Col1α2* gene and reversed dysregulated osteogenic differentiation. In contrast to OIM osteoblasts, OIM bone marrow–derived monocytes normally differentiate into mature osteoclasts, which was unaltered by the treatment with GeneRide or Cas9/GR (Figure S9). These results suggest that the *Col1α2* mutation does not affect osteoclast development. A single dose of systemically administered dual AAV9 vectors effectively delivered Cas9/GR to osteoblast-lineage cells residing in the skeleton, corrected the *Col1α2* mutation, and ameliorated OI skeletal phenotypes in OIM mice, such as spontaneous fractures, skeletal

the distance of interfemur and interischia in the pelvic bone was measured (yellow arrows, A and C, top). Kondziela scoring of AAV-treated mice was performed to assess grip strength (C, bottom). Femoral trabecular bone mass and cortical bone thickness were assessed by microCT (n = 5–6). Representative 2D reconstruction and relative quantification are displayed (D and E). Scale bars, 1 mm. Trabecular (Tra.) BV/TV and trabecular number per cubic millimeter. Cas9/GR treatment improved the low mineral density of OIM cortical bone. Longitudinal sections of AAV-treated cortical bone were stained with silver nitrate to assess morphology and dendrites of osteocytes embedded in the bone matrix. Representative images (F) and quantification of dendrite number or length (G) are displayed. Scale bars, 10 μm. mRNA levels of sclerostin (Sost) in AAV-treated tibia were measured by qPCR analysis and normalized to β-actin (n = 8–10, h). Longitudinal sections of AAV-treated femurs were stained with toluidine blue and Tartrate-resistant acid phosphatase (TRAP) to quantify the number of osteoblasts or osteoclasts per bone surface, respectively (n = 5–6). BS, bone surface; OB, osteoblast; OC, osteoclast. Gray boxes: OIM mice treated with the indicated rAAV9s. Values represent mean ± SD by 1-way ANOVA test (C, D, and G–I).

deformities, and weak grip strength. Mechanistically, AAV-mediated gene editing not only dampened bone matrix turnover rates by reducing osteoblast and osteoclast development *in vivo* but also improved the cellular network of mechano-sensing osteocytes embedded in the bone matrix, which ameliorates bone architecture, mass, and mineralization of OIM mice. Thus, these findings provide the first *in vivo* evidence that AAV-based gene editing is a promising option for treating OI.

CRISPR-Cas9-mediated gene editing permanently corrects disease-causing mutations, which is a highly desirable therapeutic option for early-onset genetic disorders such as a severe form of type III OI. However, this approach has several limitations, including immune reactions against the bacterial nuclease Cas9, off-target cleavage and mutagenesis, and induction of chromosomal aberrations. In particular, these concerns become more problematic by AAV-mediated long-term expression of Cas9. For example, prolonged expression of CRISPR-Cas9-continuously generates random DNA breaks and repairs, increasing the mosaic mutation rate.[34] To resolve these safety concerns of CRISPR-Cas9, shortening the half-life of Cas9 by tagging with ubiquitin-proteasomal degradation signals has been suggested.[35] Alternatively, a GeneRide system has been developed that uses the targeted insertion of a promoterless therapeutic cDNA into the locus without requiring Cas9. However, GeneRide-mediated gene editing via HDR is poorly efficient *in vivo* and requires the cell cycle.[17] A previous study demonstrated that the gene editing efficacy and safety profile of GeneRide in liver metabolic diseases were substantially enhanced when combined with CRISPR-Cas9,[36] which is similar to our findings in OI. However, double dosing is required for the combinatory approach of CRISPR-Cas9 and GeneRide, causing a toxicity issue. Therefore, further vector improvement to insert CRISPR-Cas9 and a shorter version of GR into a single AAV vector genome should be considered. In addition, AAV-mediated expression of SaCas9 exclusively in osteoblast-lineage cells, such as using osteoblast-specific promoters or nonskeletal tissue–specific miRNA-mediated repression in the vector genome design, will enable more precise bone-specific expression. Finally, future investigation for vector biodistribution, toxicity, dose ranging, and therapeutic efficacy in nonhuman primates is required before any consideration can be given to applying AAV gene therapy to individuals with OI.

MATERIALS AND METHODS

AAV vector design and production for expressing SaCas9 and GR

The thyroxine binding globulin (TBG) promoter in pX602-AAV-TBG::NLS-SaCas9-NLS-HA-OLLAS-bGHpA; U6::BsaI-sgRNA (Addgene plasmid no. 61593; http://n2t.net/addgene:61593; RRID: Addgene_61593) was replaced with the U1a promoter to construct pAAV-U1a-SaCas9-U6-BsaI-sgRNA plasmid. The sgRNA targeting a PAM at nucleotide 3,987–3,992 of Col1α2 was incorporated into the pAAV-U1a-SaCas9-U6-BsaI-sgRNA to generate the pAAV-U1a-SaCas9-U6-sgCol1a2 plasmid for gene editing (Figure S1B). pAAV-U1a-egfp plasmid was used as a negative control.

Gene ride

A total of 1,838 bp-size sequences to the pro-α2 C-terminal propeptide (810 bp intron, 147 bp exon including G3983 and stop codon, and 881 bp 3′ UTR) and 131 bp SV40 polyadenylation sequences were incorporated into the promoterless pAAV plasmid[37] (Figure S1B). The sequences of gBlocks for plasmid construction are found in Table S1. AAV9 was produced by transient HEK 293 cell transfection and CsCl sedimentation by the University of Massachusetts Chan Medical School Viral Vector Core, as previously described.[4] Vector preparations were determined by droplet digital PCR, and purity was assessed by 4%–12% SDS-acrylamide gel electrophoresis and silver staining (Invitrogen).

Cell lines and cell culture

For osteoblast culture, COBs or BMSCs were obtained from OIM ($Oim^{m/m}$) mice or littermate controls ($Oim^{+/+}$). Primary COBs were isolated from OIM newborn pups at postnatal days 3–5 using collagenase and dispase II and immortalized via lentivirus-mediated expression of a heat-sensitive SV40 large T antigen (generated by VectorBuilder). The cells were clonally selected to obtain homogeneous COBs. Alternatively, the femurs and tibias were surgically removed from 4-week-old OIM mice and crushed using a mortar and pestle. After removing red blood cells, BMSCs were cultured under growth medium (α-MEM medium (Gibco), 10% fetal bovine serum (FBS; Corning), 2 mM L-glutamine, 1% nonessential amino acids, and 1% penicillin/streptomycin). For osteogenic differentiation, ascorbic acid (200 μM, Sigma, A8960) and β-glycerophosphate (10 mM, Sigma, G9422) were added to the growth medium. For the ALP activity assay, osteoblasts were incubated with alamarBlue solution (Invitrogen, DAL1100) to check cell viability. Subsequently, cells were washed with PBS and incubated with a solution containing 6.5 mM Na_2CO_3, 18.5 mM $NaHCO_3$, 2 mM $MgCl_2$, and phosphatase substrate (Sigma, S0942), and ALP activity was measured by spectrometer. For ALP staining, osteoblasts were fixed with 10% neutral formalin buffer and stained with the solution containing Fast Blue (Sigma, FBS25) and Naphthol AS-MX (Sigma, 855). At day 6 of the osteogenic culture, total RNA was extracted using Qiazol (Qiagen, 79306) and subjected to qPCR analysis.

For osteoclast culture, bone marrow cells were flushed from the femurs and tibias of 2-month-old mice (C57BL/6 J) and cultured in Petri dishes in α-MEM medium with 10% FBS and 10 ng/mL of macrophage colony-stimulating factor (M-CSF; R&D Systems) to obtain bone marrow monocytes (BMMs). After 12 h, nonadherent cells were collected and replated into 24-well plates at a density of 0.5×10^6 cells/well in the same medium for 2 days. BMMs were differentiated into osteoclasts in the presence of RANKL (20 ng/mL; R&D Systems) and M-CSF (20 ng/mL; R&D Systems) for 6 days. The osteoclast differentiation medium was changed every 48 h.

Sanger sequencing, NGS, and qPCR analyses

Genomic DNA was extracted from AAV-transduced osteoblasts, liver, muscle, or femur/tibia, PCR amplified, and subjected to Sanger

sequencing or NGS analysis. For NGS analysis, the cDNAs synthesized from cellular or tissue genomic DNA were amplified using Col1α2-targeting primers and the PCR products were subjected to NGS in the Massachusetts General Hospital Center for Computational & Integrative Biology DNA Core. For qPCR, total RNA was extracted from AAV-transduced cells or femur and mRNA levels of the corrected *Col1α2* gene were assessed by qPCR analysis and normalized to β-actin. Primer sequences are provided in Table S2.

Mice

OIM mice[23] were purchased from The Jackson Laboratory and maintained on a C57BL/6 background. Mouse genotypes were determined by PCR on tail genomic DNA. Briefly, the phenotyping strategy was adapted from the previous study.[38] The primers are 5′-ACTGTCTGTCTACAGTGAACGTCTTAA T-3′ outer forward, 5′-GATGTAGATGCATAGAAGACATGGAAGG-3′ outer reverse, 5′-TTCCCATTTTTTTCTATTATACAGAAACAG-3′ inner forward (WT specific), and 5′-AATGATTGTCTTGCCCCATTCATTTTTT-3′ inner reverse (OIM specific), which flank the single nucleotide deletion. The PCR program is as follows: 94°C for 2 min, then 30 cycles of 94°C for 30 s, 60°C for 30 s, 72°C for 30 s, and lastly, 72°C for 5 min. The product sizes are internal control (440 bp), WT (303 bp), and OIM (195 bp). All of the animals were used in accordance with the *NIH Guide for the Care and Use of Laboratory Animals* and were handled according to protocols approved by the University of Massachusetts Chan Medical School's Institutional Animal Care and Use Committee.

The experiments were carried out on OIM mice and littermate controls. One-month-old mice were randomly divided into six groups (PBS, AAV9.egfp, AAV9.NTC, AAV9.SaCas9, AAV9.GR, and AAV9.Cas9/GR) and i.v. injected with a single dose of AAV9.NTC (100 μL of 5×10^{12} genome copies (GC)/mL), AAV9.SaCas9 (100 μL of 5×10^{12} GC/mL), AAV9.GR (100 μL of 5×10^{12} GC/mL), or AAV9.GR (50 μL of 10^{13} GC/mL) + AAV9.Cas9 (50 μL of 10^{13} GC/mL) at a concentration of 2.5×10^{13} vg/kg.[10,11,39] Four weeks later, mice were euthanized and the biodistribution of AAV in individual tissues was assessed by GFP expression using the IVIS-100 optical imaging system, qRT-PCR analysis, and fluorescence microscopy cryo-sectioned tissues. In addition, genomic DNA or RNA was isolated, PCR amplified, and subjected to Sanger sequencing, NGS, and qRT-PCR analysis. Eight weeks after AAV injection, mice were placed on an inverted screen, and Kondziela scoring was performed to examine grip strength. The Kondziela test measures the muscle strength of all four limbs using the inverted screen.[28,29] For skeletal analysis, radiography analysis of the whole body, microCT and histologic analyses of femurs, and qRT-PCR analysis of tibial RNA were performed.

Clinical scoring of OI skeletal phenotypes

Euthanized mice were processed for radiographic (two-dimensional [2D] images) and microCT (3D images) analyses of the whole body to perform a clinical assessment of OI skeletal phenotypes. Each mouse was independently scored by a minimum of two researchers, blinded as to the identity of the groups, and each score was recorded. Any skeletal deformity and fracture at the target site were scored as a point "1" (without consideration of severity) to highlight the incident frequency.

MicroCT analysis

MicroCT of femur bones was carried out using microCT 35 (Scanco Medical) as previously reported, to carry out qualitative and quantitative assessments of trabecular bone microarchitecture.[10] Briefly, femurs dissected from the indicated mice groups were fixed with 10% neutral buffered formalin and scanned using a microCT 35 with a spatial resolution of 7 μm. For trabecular bone analysis of the distal femur, an upper 2.1-mm region beginning 280 μm proximal to the growth plate was contoured. The 3D reconstruction images were obtained from contoured 2D images by methods based on the distance transformation of the binarized images. Alternatively, the Inveon multimodality 3D visualization program was used to generate fused 3D viewing of multiple static or dynamic volumes of microCT modalities (Siemens Medical Solutions). Trabecular bone parameters (i.e., bone volume/tissue volume ratio [BV/TV] and trabecular number) were calculated. For cortical bone analysis of the femur, a mid-shaft region of 0.6 mm in length was used. All of the images presented are representative of the respective genotypes (n = 6).

Histology and immunofluorescence

Femurs were dissected from AAV-treated mice for histological studies. Briefly, femurs were fixed in 10% neutral buffered formalin for 2 days, followed by decalcification for 2–4 weeks using 0.5 M tetrasodium EDTA. Furthermore, tissues were dehydrated by passage through an ethanol series, cleared twice in xylene, embedded in paraffin, and sectioned at a thickness of 6 μm along the coronal plate from anterior to posterior. Decalcified femoral sections were stained with silver nitrate.

For immunofluorescence, the femoral bone was fixed with 4% paraformaldehyde for 2 days and decalcified in 0.5 M tetrasodium EDTA solution for 10 days. Semidecalcified samples were infiltrated with 25% sucrose phosphate for 4 days. All of the samples were embedded in a 50/50 mixture of 25% sucrose solution and OCT compound (Sakura) and cut into 12-μm-thick sagittal sections using a cryostat (Leica). Nuclei were stained with DAPI. An Olympus IX81confocal microscope was used to image samples.

Statistical analysis

Except where indicated, all of the data are graphically represented as the mean ± SD. For experiments with three or more samples, statistical analysis was performed using one-way ANOVA followed by a Bonferroni-corrected Student's t test. For two-sample comparisons, a two-tailed, unpaired Student's t test was applied. Values were considered statistically significant at $p < 0.05$. The results shown are representative of three or more individual experiments.

DATA AND CODE AVAILABILITY

Data supporting the findings of this paper are available from the corresponding author upon reasonable request.

SUPPLEMENTAL INFORMATION

Supplemental information can be found online at https://doi.org/10.1016/j.omtn.2023.102111.

ACKNOWLEDGMENTS

We thank Dr. Jung-Min Kim, Ms. Zhihao Chen, and Ms. Agustina Rodriguez for technical support; Drs. Marelise Eekhoff and Dimitra Micha for discussions; Dr. Melanie Trombly for editing the manuscript; and Dr. Wang Dan for providing the pAAV.U1a.SaCas9 plasmid. We also thank the many individuals who provided valuable reagents. This project was supported by AAVAA Therapeutics. G.G. receives grants under the NIH, United States (R01NS076991, P01HL131471, R01AI121135, UG3HL147367, R01HL097088, R01HL152723, U19AI149646, and UH3HL147367).

AUTHOR CONTRIBUTIONS

Y.-S.Y. designed, executed, and interpreted the experiments. T.S. and S.C. performed the *in vitro* experiments. H.M. and J.X. designed and generated all of the AAVs used in this work. J.X., G.G., and J.-H.S. supervised the research and prepared the manuscript.

DECLARATION OF INTERESTS

Y.-S.Y., S.C., J.X., G.G., and J.-H.S. have submitted a patent application concerning the methodology described in this study. G.G. and J.-H.S. are scientific cofounders of AAVAA Therapeutics and hold equity in this company. G.G. is also a scientific cofounder of Adrenas Therapeutics, Voyager Therapeutics, and Aspa Therapeutics and holds equity in these companies. G.G. is an inventor on patents with potential royalties licensed to Adrenas Therapeutics, Voyager Therapeutics, Aspa Therapeutics, and other biopharmaceutical companies.

REFERENCES

1. Martin, E., and Shapiro, J.R. (2007). Osteogenesis imperfecta:epidemiology and pathophysiology. Curr. Osteoporos. Rep. *5*, 91–97.
2. Marini, J.C., Forlino, A., Bächinger, H.P., Bishop, N.J., Byers, P.H., Paepe, A.D., Fassier, F., Fratzl-Zelman, N., Kozloff, K.M., Krakow, D., et al. (2017). Osteogenesis imperfecta. Nat. Rev. Dis. Primers *3*, 17052.
3. Rossi, V., Lee, B., and Marom, R. (2019). Osteogenesis imperfecta: advancements in genetics and treatment. Curr. Opin. Pediatr. *31*, 708–715.
4. Palomo, T., Vilaça, T., and Lazaretti-Castro, M. (2017). Osteogenesis imperfecta: diagnosis and treatment. Curr. Opin. Endocrinol. Diabetes Obes. *24*, 381–388.
5. Rousseau, J., Gioia, R., Layrolle, P., Lieubeau, B., Heymann, D., Rossi, A., Marini, J.C., Trichet, V., and Forlino, A. (2014). Allele-specific Col1a1 silencing reduces mutant collagen in fibroblasts from Brtl mouse, a model for classical osteogenesis imperfecta. Eur. J. Hum. Genet. *22*, 667–674.
6. Lindahl, K., Kindmark, A., Laxman, N., Åström, E., Rubin, C.J., and Ljunggren, Ö. (2013). Allele dependent silencing of collagen type I using small interfering RNAs targeting 3'UTR Indels - a novel therapeutic approach in osteogenesis imperfecta. Int. J. Med. Sci. *10*, 1333–1343.
7. Yin, H., Kanasty, R.L., Eltoukhy, A.A., Vegas, A.J., Dorkin, J.R., and Anderson, D.G. (2014). Non-viral vectors for gene-based therapy. Nat. Rev. Genet. *15*, 541–555.
8. Asokan, A., Schaffer, D.V., and Samulski, R.J. (2012). The AAV vector toolkit: poised at the clinical crossroads. Mol. Ther. *20*, 699–708.
9. Vandenberghe, L.H., Wilson, J.M., and Gao, G. (2009). Tailoring the AAV vector capsid for gene therapy. Gene Ther. *16*, 311–319.
10. Yang, Y.S., Xie, J., Wang, D., Kim, J.M., Tai, P.W.L., Gravallese, E., Gao, G., and Shim, J.H. (2019). Bone-targeting AAV-mediated silencing of Schnurri-3 prevents bone loss in osteoporosis. Nat. Commun. *10*, 2958.
11. Oh, W.T., Yang, Y.S., Xie, J., Ma, H., Kim, J.M., Park, K.H., Oh, D.S., Park-Min, K.H., Greenblatt, M.B., Gao, G., and Shim, J.H. (2023). WNT-modulating gene silencers as a gene therapy for osteoporosis, bone fracture, and critical-sized bone defects. Mol. Ther. *31*, 435–453.
12. Mali, P., Yang, L., Esvelt, K.M., Aach, J., Guell, M., DiCarlo, J.E., Norville, J.E., and Church, G.M. (2013). RNA-guided human genome engineering via Cas9. Science *339*, 823–826.
13. Cong, L., Ran, F.A., Cox, D., Lin, S., Barretto, R., Habib, N., Hsu, P.D., Wu, X., Jiang, W., Marraffini, L.A., and Zhang, F. (2013). Multiplex genome engineering using CRISPR/Cas systems. Science *339*, 819–823.
14. Sander, J.D., and Joung, J.K. (2014). CRISPR-Cas systems for editing, regulating and targeting genomes. Nat. Biotechnol. *32*, 347–355.
15. Wang, M., Glass, Z.A., and Xu, Q. (2017). Non-viral delivery of genome-editing nucleases for gene therapy. Gene Ther. *24*, 144–150.
16. Qiu, M., Glass, Z., Chen, J., Haas, M., Jin, X., Zhao, X., Rui, X., Ye, Z., Li, Y., Zhang, F., and Xu, Q. (2021). Lipid nanoparticle-mediated codelivery of Cas9 mRNA and single-guide RNA achieves liver-specific in vivo genome editing of Angptl3. Proc. Natl. Acad. Sci. USA *118*, e2020401118.
17. Barzel, A., Paulk, N.K., Shi, Y., Huang, Y., Chu, K., Zhang, F., Valdmanis, P.N., Spector, L.P., Porteus, M.H., Gaensler, K.M., and Kay, M.A. (2015). Promoterless gene targeting without nucleases ameliorates haemophilia B in mice. Nature *517*, 360–364.
18. Senís, E., Fatouros, C., Große, S., Wiedtke, E., Niopek, D., Mueller, A.K., Börner, K., and Grimm, D. (2014). CRISPR/Cas9-mediated genome engineering: an adeno-associated viral (AAV) vector toolbox. Biotechnol. J. *9*, 1402–1412.
19. Wang, D., Li, J., Song, C.Q., Tran, K., Mou, H., Wu, P.H., Tai, P.W.L., Mendonca, C.A., Ren, L., Wang, B.Y., et al. (2018). Cas9-mediated allelic exchange repairs compound heterozygous recessive mutations in mice. Nat. Biotechnol. *36*, 839–842.
20. Bengtsson, N.E., Hall, J.K., Odom, G.L., Phelps, M.P., Andrus, C.R., Hawkins, R.D., Hauschka, S.D., Chamberlain, J.R., and Chamberlain, J.S. (2017). Muscle-specific CRISPR/Cas9 dystrophin gene editing ameliorates pathophysiology in a mouse model for Duchenne muscular dystrophy. Nat. Commun. *8*, 14454.
21. Pihlajaniemi, T., Dickson, L.A., Pope, F.M., Korhonen, V.R., Nicholls, A., Prockop, D.J., and Myers, J.C. (1984). Osteogenesis imperfecta: cloning of a pro-alpha 2(I) collagen gene with a frameshift mutation. J. Biol. Chem. *259*, 12941–12944.
22. Pace, J.M., Wiese, M., Drenguis, A.S., Kuznetsova, N., Leikin, S., Schwarze, U., Chen, D., Mooney, S.H., Unger, S., and Byers, P.H. (2008). Defective C-propeptides of the proalpha2(I) chain of type I procollagen impede molecular assembly and result in osteogenesis imperfecta. J. Biol. Chem. *283*, 16061–16067.
23. Chipman, S.D., Sweet, H.O., McBride, D.J., Jr., Davisson, M.T., Marks, S.C., Jr., Shuldiner, A.R., Wenstrup, R.J., Rowe, D.W., and Shapiro, J.R. (1993). Defective pro alpha 2(I) collagen synthesis in a recessive mutation in mice: a model of human osteogenesis imperfecta. Proc. Natl. Acad. Sci. USA *90*, 1701–1705.
24. Nicholls, A.C., Osse, G., Schloon, H.G., Lenard, H.G., Deak, S., Myers, J.C., Prockop, D.J., Weigel, W.R., Fryer, P., and Pope, F.M. (1984). The clinical features of homozygous alpha 2(I) collagen deficient osteogenesis imperfecta. J. Med. Genet. *21*, 257–262.
25. Ran, F.A., Cong, L., Yan, W.X., Scott, D.A., Gootenberg, J.S., Kriz, A.J., Zetsche, B., Shalem, O., Wu, X., Makarova, K.S., et al. (2015). In vivo genome editing using Staphylococcus aureus Cas9. Nature *520*, 186–191.
26. Gioia, R., Panaroni, C., Besio, R., Palladini, G., Merlini, G., Giansanti, V., Scovassi, I.A., Villani, S., Villa, I., Villa, A., et al. (2012). Impaired osteoblastogenesis in a murine model of dominant osteogenesis imperfecta: a new target for osteogenesis imperfecta pharmacological therapy. Stem Cell. *30*, 1465–1476.

27. Wang, D., Tai, P.W.L., and Gao, G. (2019). Adeno-associated virus vector as a platform for gene therapy delivery. Nat. Rev. Drug Discov. *18*, 358–378.

28. Kondziella, W. (1964). [a New Method for the Measurement of Muscle Relaxation in White Mice]. Arch. Int. Pharmacodyn. Ther. *152*, 277–284.

29. Deacon, R.M. (2013). Measuring the strength of mice. J. Vis. Exp. *76*, 2610.

30. Komor, A.C., Kim, Y.B., Packer, M.S., Zuris, J.A., and Liu, D.R. (2016). Programmable editing of a target base in genomic DNA without double-stranded DNA cleavage. Nature *533*, 420–424.

31. Anzalone, A.V., Randolph, P.B., Davis, J.R., Sousa, A.A., Koblan, L.W., Levy, J.M., Chen, P.J., Wilson, C., Newby, G.A., Raguram, A., and Liu, D.R. (2019). Search-and-replace genome editing without double-strand breaks or donor DNA. Nature *576*, 149–157.

32. Zetsche, B., Gootenberg, J.S., Abudayyeh, O.O., Slaymaker, I.M., Makarova, K.S., Essletzbichler, P., Volz, S.E., Joung, J., van der Oost, J., Regev, A., et al. (2015). Cpf1 is a single RNA-guided endonuclease of a class 2 CRISPR-Cas system. Cell *163*, 759–771.

33. Ran, F.A., Hsu, P.D., Lin, C.Y., Gootenberg, J.S., Konermann, S., Trevino, A.E., Scott, D.A., Inoue, A., Matoba, S., Zhang, Y., and Zhang, F. (2013). Double nicking by RNA-guided CRISPR Cas9 for enhanced genome editing specificity. Cell *154*, 1380–1389.

34. Yen, S.T., Zhang, M., Deng, J.M., Usman, S.J., Smith, C.N., Parker-Thornburg, J., Swinton, P.G., Martin, J.F., and Behringer, R.R. (2014). Somatic mosaicism and allele complexity induced by CRISPR/Cas9 RNA injections in mouse zygotes. Dev. Biol. *393*, 3–9.

35. Tu, Z., Yang, W., Yan, S., Yin, A., Gao, J., Liu, X., Zheng, Y., Zheng, J., Li, Z., Yang, S., et al. (2017). Promoting Cas9 degradation reduces mosaic mutations in non-human primate embryos. Sci. Rep. *7*, 42081.

36. De Caneva, A., Porro, F., Bortolussi, G., Sola, R., Lisjak, M., Barzel, A., Giacca, M., Kay, M.A., Vlahoviček, K., Zentilin, L., and Muro, A.F. (2019). Coupling AAV-mediated promoterless gene targeting to SaCas9 nuclease to efficiently correct liver metabolic diseases. JCI Insight *5*, e128863.

37. Xie, J., Ameres, S.L., Friedline, R., Hung, J.H., Zhang, Y., Xie, Q., Zhong, L., Su, Q., He, R., Li, M., et al. (2012). Long-term, efficient inhibition of microRNA function in mice using rAAV vectors. Nat. Methods *9*, 403–409.

38. Zimmerman, S.M., Heard-Lipsmeyer, M.E., Dimori, M., Thostenson, J.D., Mannen, E.M., O'Brien, C.A., and Morello, R. (2018). Loss of RANKL in osteocytes dramatically increases cancellous bone mass in the osteogenesis imperfecta mouse (oim). Bone Rep. *9*, 61–73.

39. Yang, Y.S., Xie, J., Chaugule, S., Wang, D., Kim, J.M., Kim, J., Tai, P.W.L., Seo, S.K., Gravallese, E., Gao, G., and Shim, J.H. (2020). Bone-Targeting AAV-Mediated Gene Silencing in Osteoclasts for Osteoporosis Therapy. Mol. Ther. Methods Clin. Dev. *17*, 922–935.